HHS Public Access

Author manuscript

Proc IEEE Int Symp Biomed Imaging. Author manuscript; available in PMC 2017 April 06.

Published in final edited form as:

Proc IEEE Int Symp Biomed Imaging. 2012 May ; 2012: 178–181. doi:10.1109/ISBI.2012.6235513.

Development of a novel 2D color map for interactive segmentation of histological images

Qaiser Chaudry[1], **Yachna Sharma**[1], **Syed H. Raza**[1], and **May D. Wang**[2]

[1]Department of Electrical & Computer Engineering, Georgia institute of Technology, Atlanta, GA, USA

[2]The Wallace H. Coulter Department of Biomedical Engineering, Georgia Institute of Technology and Emory University, Atlanta, GA, USA

Abstract

We present a color segmentation approach based on a two-dimensional color map derived from the input image. Pathologists stain tissue biopsies with various colored dyes to see the expression of biomarkers. In these images, because of color variation due to inconsistencies in experimental procedures and lighting conditions, the segmentation used to analyze biological features is usually ad-hoc. Many algorithms like K-means use a single metric to segment the image into different color classes and rarely provide users with powerful color control. Our 2D color map interactive segmentation technique based on human color perception information and the color distribution of the input image, enables user control without noticeable delay. Our methodology works for different staining types and different types of cancer tissue images. Our proposed method's results show good accuracy with low response and computational time making it a feasible method for user interactive applications involving segmentation of histological images.

INTRODUCTION

Segmentation of colored images is a classic problem in digital image processing. Images with sharp color distinctions can be easily segmented by using one of several segmentation algorithms available [1]. However, natural and biological stained color images lack high contrast discontinuities. In addition, there are variations among staining colors or light conditions. Thus, using computers to conduct color quantification becomes increasingly important in clinical diagnosis, and emerges as a new field called Computer Assisted Diagnosis (CAD). One of the challenges in CAD is how to perform precise color segmentation as perceived by humans.

In gray-scale image segmentation, discontinuity-based techniques [2] [3] [4], partition an image by detecting isolated points, lines and edges caused by sudden changes in gray levels. Homogeneity-based methods perform thresholding, clustering, region growing, and region splitting and merging [4]. Color is a feature of an object's surface. Distinctive colors form peaks in color histograms. Because color images are usually measured and represented by three color components: red green and blue, (R,G,B), most color segmentation approaches just extend 1-color gray intensity processing to 3-colors [3], and are generally based on either histograms or clustering techniques. In clustering-based techniques, pixels are

grouped based on a distance metric and the color values of the points. The spread within a cluster is mainly determined by color variations due to shading and device noise. An example is the K-means algorithm, which iteratively computes each cluster's membership and mean color values until convergence. In general, the K-means algorithm suffers from the local minima problem and being an un-supervised algorithm lack user control. In [1][5], the authors have shown that K-means clustering with user-provided seed points can result in better segmentation when compared to fully automated "unsupervised" K-means. Generally, clinical applications prefer accuracy over automation, if the segmentation results with user interaction can be produced in real time; they will be the top design choice. Under this guideline, i.e. to maximize the user feedback while performing the computation in real time, we have designed a color visualization and segmentation system.

Due to the complexity and heterogeneity of biomedical images, generic solutions are quite uncommon. A survey of biomedical image processing reveals a number of application-specific color segmentation techniques [6] [7] [8]. The user's perception is another important aspect for any color segmentation technique. The color models and the differentiation metric, incorporating human perception models, to separate different classes are preferred by the user as it co-relates results more closely to their knowledge base. A perceptual color segmentation algorithm [9] segmenting RGB color space into ten color categories using Munsell and CIELUV color models and dominant color detection in an image by finding ridges in the color distribution [10] are examples of incorporating human perception models to achieve better segmentation. The user's perception of color can also be incorporated by introducing interactivity and user feedback. Interactive segmentation [11], in which the "user is in the segmentation loop," allows the addition and removal of regions of interest by the user and user selected seed points segmentation [12] are the few examples.

We designed our color segmentation tool to be interactive and to incorporate color constancy perceived by humans. In addition, it offers visualization of 3D RGB colors in a 2D space that covers the pixel frequency, color composition and color class clustering (co-localization) of the images, selecting several color class samples in a time frame equivalent to single seed point selection, enhanced user control and compatibility with different types of cancer images stained with different colored dyes.

METHODS

Segmentation in color space is challenging because it is not easy to find a similarity metric that translates the user's perception of 3D color space to a single dimension decision parameter. Even with high-speed computer graphics, it is difficult for users to select or encapsulate clusters directly in a 3D space, such as the RGB space. In this work, we reduce this complexity to provide an interactive environment in 2D. For data visualization we used Hue (H) and Saturation (S) plane as mapping space where all the pixels in the test image are mapped close to other pixels which have similar HS values (co-localization). It may be noted that the color space is not being used to do the dimensionality reduction. It is only used to co-localize the pixels e.g. using HS plane, all pixels with same Hue and Saturation values will be mapped close to each other irrespective of intensity. The pixels displayed will still appear with their original intensity value i.e. the pixels in color map show all components

(RGB). We tested different visualization schemes using different images and selected HS plane for color maps as it showed better spread and easier interaction. One such example is shown in Figure 1.

Direct mapping of the pixels to visualization space has certain limitations. Because most image formats support 24-bit color values, the probability of multiple pixels mapping to a single location is significant. In addition, if the visualization space image size is large in comparison to only 255 (8 bit) possible values along one axis, blank rows and columns remain, as shown in Figure 2. We can also see that Figure 2 does not give a true representation of how frequently a specific shade of color is represented in the input image. We tried different methods to generate color map by arranging pixels in order to present the user with a true representative of the image in real time for interactive visualization. We came up with this technique termed as ‘Random Spread Visualization’ which is non-iterative method and fast enough (<30 sec) for real time visualization and interaction.

2.1. Random Spread Visualization

2D visualization shown in Figure 2 loses the information of all the pixels which map to same location. If these pixels are mapped to the empty places in the near vicinity, the color map generated in such a manner, gives a better representation of pixel co-localization and frequency of occurrence. To achieve this, rather than finding an empty location for every pixel, which is a computationally intensive operation, each pixel is mapped to a location with a random offset which is approximately 5% of the color map largest dimension. The offset is small enough so that the pixels belonging to a similar class are mapped close to each other. Few pixels may overwrite others but the zones of frequently occurring pixels filling earlier than others can be seen as a measure of co-localization. Figure 3 displays the original image and the spread of pixels in the corresponding visualization scheme. This visualization scheme is limited in displaying the true frequency of pixels, but area, along with the pixel density (compactness of color map), represents how frequently pixels of the similar color occur in the input image. For example, the scarcity of red and purple color in the input image, as compared to pink and yellow color, is demonstrated by the thick localization of pink and yellowish color in Figure 3(b).

The users are presented with this 2D color space visualization of (Figure 3b) to approximately mark the areas (Figure 3c), using the mouse, where pixels should be grouped together as a single color class. This zone marking is then used to segment the color image. The segmented image (Figure 3d) is completely dependent on the color ranges specified. Closed curves of any shape and size are acceptable and any number of color ranges can be specified, thus providing user flexibility.

To compare the segmentation results based on our color map we used level sets algorithm and few semi-supervised variants of K-means algorithm. We provide a brief description of these methods before presenting the segmentation results.

2.2. K-means Variants

Seeded K-means (SK-means) is our semi supervised variant for standard K-means [13]. Standard K-means is an unsupervised algorithm. Even initializing the algorithm with seeds

points may help early convergence but resulting final classification may not be anywhere close to starting seed points or the user's perception. SK-means utilizes user provided seed points for mean initialization as well as anchor point to restrict excessive mean movement to incorporate user's perception. During the iterative processes of mean computation, association of each point is determined based on its distance from new mean as well as starting seed point.

In SK-means, we split N data points $x^{(n)}$, in an I dimensional space, into K clusters with means $m^{(k)}$ and initial seed points $s^{(k)}$. Each vector x has I components x_i and its distance from kth mean and kth seed point is given by

$$d_k^{(n)} = \sqrt{\sum_i (x_i^{(n)} - m_i^{(k)})^2} + \sqrt{\sum_i (x_i^{(n)} - s_i^{(k)})^2}$$

At start of SK-means, all means $m^{(k)}$ are assigned seed point values $s^{(k)}$ *i.e.* $m^{(k)}=s^{(k)}$. In the assignment step, each data point n is assigned to the nearest cluster based on minimization $d_{(n)k}$ which includes both the distance from the current cluster mean and the cluster seed point. The new assignment of clusters for all points is given by

$$\hat{C}(n) = \underset{k}{argmin} \left\{ d_k^{(n)} \right\}, \quad r_k^{(n)} = \left\{ \begin{array}{ll} 1 & if \quad \hat{C}(n)=k \\ 0 & if \quad \hat{C}(n) \neq k \end{array} \right\}$$

All the data points $x_{(n)}$assigned to a cluster C form part of its responsibility and is given by the responsibility indicator *r*.

In update step the updated means are computed as

$$m^{(k)} = \frac{\sum_n r_k^{(n)} x^{(n)}}{\sum_n r_k^{(n)}}$$

Repeat the assignment step and update step until the change in mean assignment is below a threshold.

Multi-seeded K-means (MSK-means) is similar to SK-means except that each class is subdivided into multiple subclasses. This helps in better user feedback by providing more number of seed points (one per subclass). Intra-class variations can be captured by corresponding variation in the selected seed points. After the classification process the subclasses are merged back to generate main class labels.

Weighted SK-means (WSK-means) variant of SK-means allows user to change the classification results with the help of sliders bars in a GUI. The original equation of SK-means is modified as

$$d_k^{(n)} = W_k \left(\sqrt{\sum_i (x_i^{(n)} - m_i^{(k)})^2} + \sqrt{\sum_i (x_i^{(n)} - s_i^{(k)})^2} \right)$$

where W_k is the weight parameter adjusted by the slider control.

The user keeps manipulating the sliders controls visualizing the segmentation results in real time until desired results are achieved.

A better comparison of the aforementioned algorithms can be done using the visualization in Figure 4. It may be noted that in actual practice all algorithms except color map utilize 3D space for classification.

TESTING AND COMPARISONS

To best of our knowledge, no histological image data is available where each pixel is labeled that can be used as a ground truth for testing different algorithms. In the absence of such a dataset, we tested our algorithm for H&E, IHC stained biopsy tissue images of renal cell carcinoma and head & neck cancer. We devised a strategy to compare the accuracies of afore mentioned algorithms. We consider WSK-means algorithm results as a reference, in the absence of ground truth, since it provides interface to the user to update classification results until the best perceived segmentation is achieved. To support our decision, we used the level sets algorithm as the second reference. Our level sets implementation, based on the gray level intensity cost function, is suited best to segment the dark stained nuclei in the image. Comparing only this class we were able to show that accuracies above 95% can be obtained which are close to optimum as the two algorithms inherently differ from each other.

Having verified our reference results, we used them to conduct a human interaction study to compare the performance and accuracy of other algorithms under consideration. Our study involved eight users with varying background from new to frequent users of histology images. We used six H&E stained images of Renal Cell Carcinoma (RCC) images which were divided in two groups of 512×512 and 1024×1024 pixels to compare the variation in computational cost with image size. The users were presented with the previously described 2D color space visualization of (Figure 3b) and were prompted to approximately mark the areas where pixels can be grouped together as a single color class. For SK-means, the users mark seed points on the test image which best represents each class while in MSK-means user select multiple seeds per class to capture intra-class variation. The user interaction time including computational time of all the algorithms was recorded and all the algorithms were compared for performance and accuracy.

RESULTS AND DISCUSSION

The performance results (Table-1 and Figure 5) show that random spread color map is faster than MSK-means and the average time taken by the user is less than 30 seconds per image, which is reasonable for most applications. Color map performance advantage, being a non-iterative algorithm, becomes apparent when the image size becomes large. The

computational time for both SK-means and MSK-means time nearly doubled for larger images and only increased fractionally in case of color map segmentation.

To compare accuracy of segmented images either region-based or pixel-based metrics are used [14]. In our image data we are interested in texture information inside the objects (nuclei) so we compared pixel labels from each segmented image. We used class accuracy, commission error and omission error as our evaluation metrics. The segmentation accuracy results are shown in table-2. As mentioned earlier WSK-means was used as reference validated by best level sets segmentation results selected after processing at various intensity thresholds. It can be seen that MSK-means performs better than SK-means as expected and color maps showed even better accuracies than MSK-means. Further analysis showed that accuracies are also dependent on type of the image as well as user's training and practice. It was observed that trained user can use the tool to get better accuracies especially in case of color maps based segmentation. The control available in color maps helps in achieving better segmentation than other algorithms as highlighted in Figure 6.

We have tested our algorithm for H&E, IHC stained biopsy tissue images but our segmentation approach is applicable to other types of staining. In addition, our methodology presents important image statistics in a user friendly way. For example, the color spread provides three useful features of an image: its component colors, amount of each color and most importantly co-localization or neighborhood information about color. Since we are presenting the 3D HSV color model with only two dimensions we necessarily discard intensity in the model resulting in the co-localization of black, gray and white at the center of the visualization. Even with this limitation, we have shown that proper visualization of the component colors along with user interactivity results in better segmentation results. Our segmentation scheme is particularly useful for biological images since conventional schemes do not cater to the gradual color variations in these images. Moreover, the algorithm is iteration-free and executes faster than conventional K-means and its variants. Our segmentation tool is semi-automatic to capture miniscule color details. With our previous experience in the field, we see prospects of this work towards use of quantitative analysis and study of different types of histological images.

Acknowledgments

We would like to acknowledge the efforts of Dr. Andrew N. Young for providing us the imaging data and providing valuable information for interpretation of the results from pathological perspective. We would like to thank Dr. Richard Moffitt, Dr. Mitchell Parry, Dr. Todd Stokes and Dr. John Phan for their valuable feedback through various stages of this work.

References

1. Waheed S, Moffitt R, Chaudry Q, et al. Computer Aided Histopathological Classification of Cancer Subtypes. BIBE. 2007:503–508.
2. Fu K, Mui J. A survey on image segmentation. Pattern Recognition. 1981; 13(1):3–16.
3. Haralick R, Shapiro L. Image segmentation techniques. Computer vision, graphics, and image processing. 1985; 29(1):100–132.
4. Pal N, Pal S. A review on image segmentation techniques. Pattern Recognition. 1993; 26(9):1277–1294.
5. Arthur D, Vassilvitskii S. k-means++: The advantages of careful seeding. 2007:1027–1035.

6. Umbaugh S, Moss R, Stoecker W, et al. Automatic color segmentation algorithms-with application to skin tumor feature identification. IEEE Engineering in Medicine and Biology Magazine. 1993; 12(3):75–82.
7. Gejgus P, Placek J. Skin color segmentation method based on mixture of gaussians and its application in learning system for finger alphabet. CompSysTech. 2004:1–6.
8. Fang Y, Tan T. A novel adaptive colour segmentation algorithm and its application to skin detection. BMVC. 2000:23–31.
9. Schmid P, Fischer S. Colour segmentation for the analysis of pigmented skin lesions. ICIP. 2002:688–692.
10. Healey C, Enns J. A perceptual colour segmentation algorithm. Tech Rep. 1996
11. Gao J, Kosaka A, Kak A. Interactive color image segmentation editor driven by active contour model. ICIP. 2002:245–249.
12. Maxwell B. A Physics-Based Approach to Interactive Segmentation. LNCS. 1999:656–656.
13. MacKay, D. Information Theory, Pattern Recognition and Neural Networks. Cambridge University Press; 2003.
14. Haindl, M., Mikes, S. Texture segmentation benchmark. http://mosaic.utia.cas.cz/

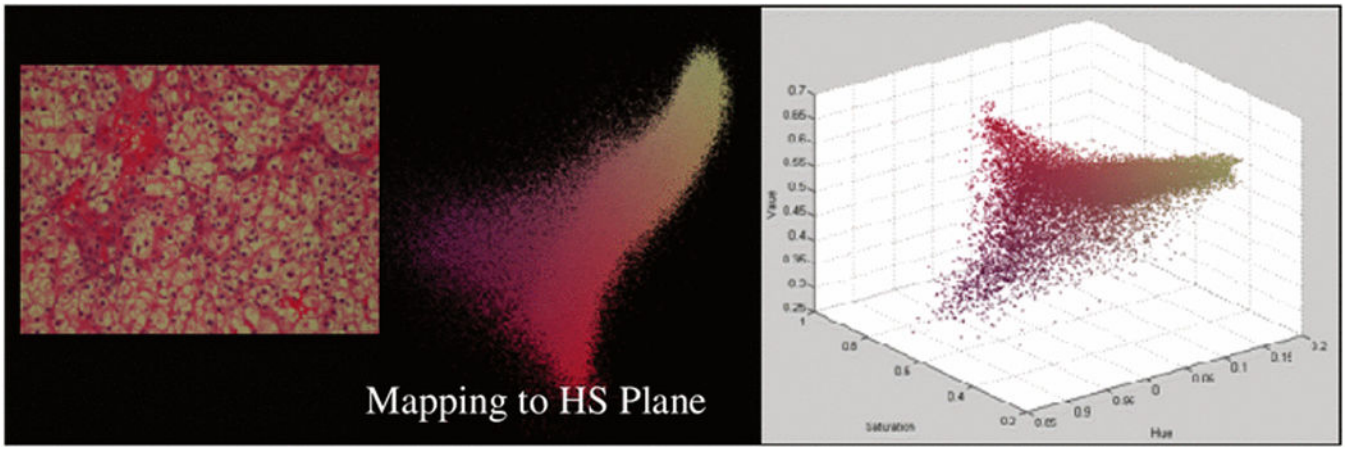

Figure 1.
Mapping of image pixels to HS plane using random spread visualization showing a good representation of image pixels 3D scatter plot.

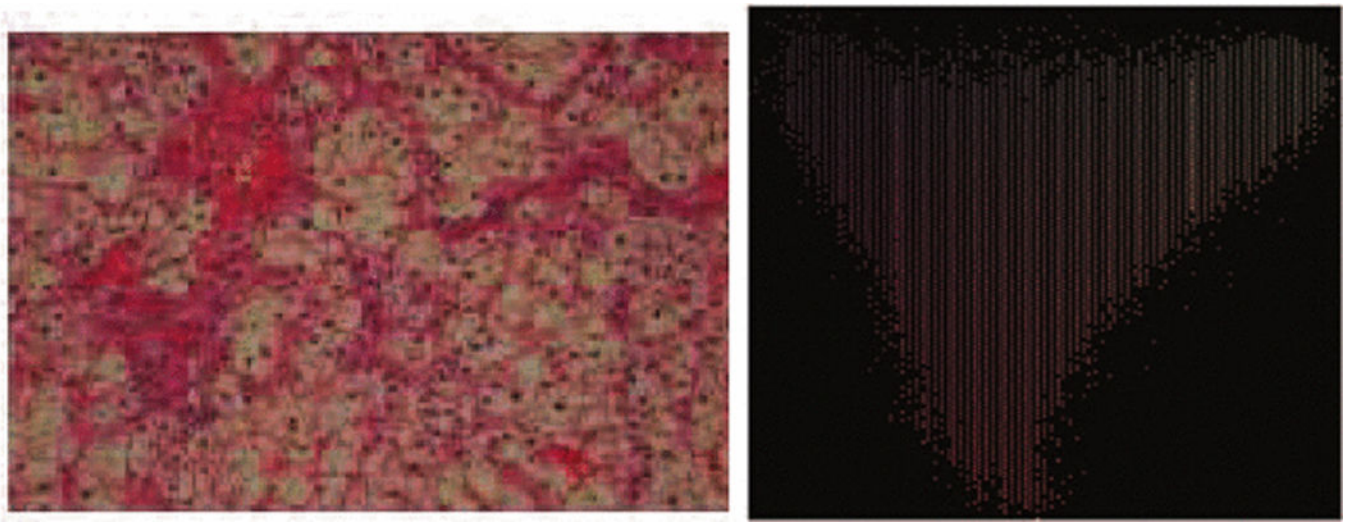

Figure 2.
Test image and its 2D Visualization space representation. Both the problems of co-located pixels and the unmapped space can be seen.

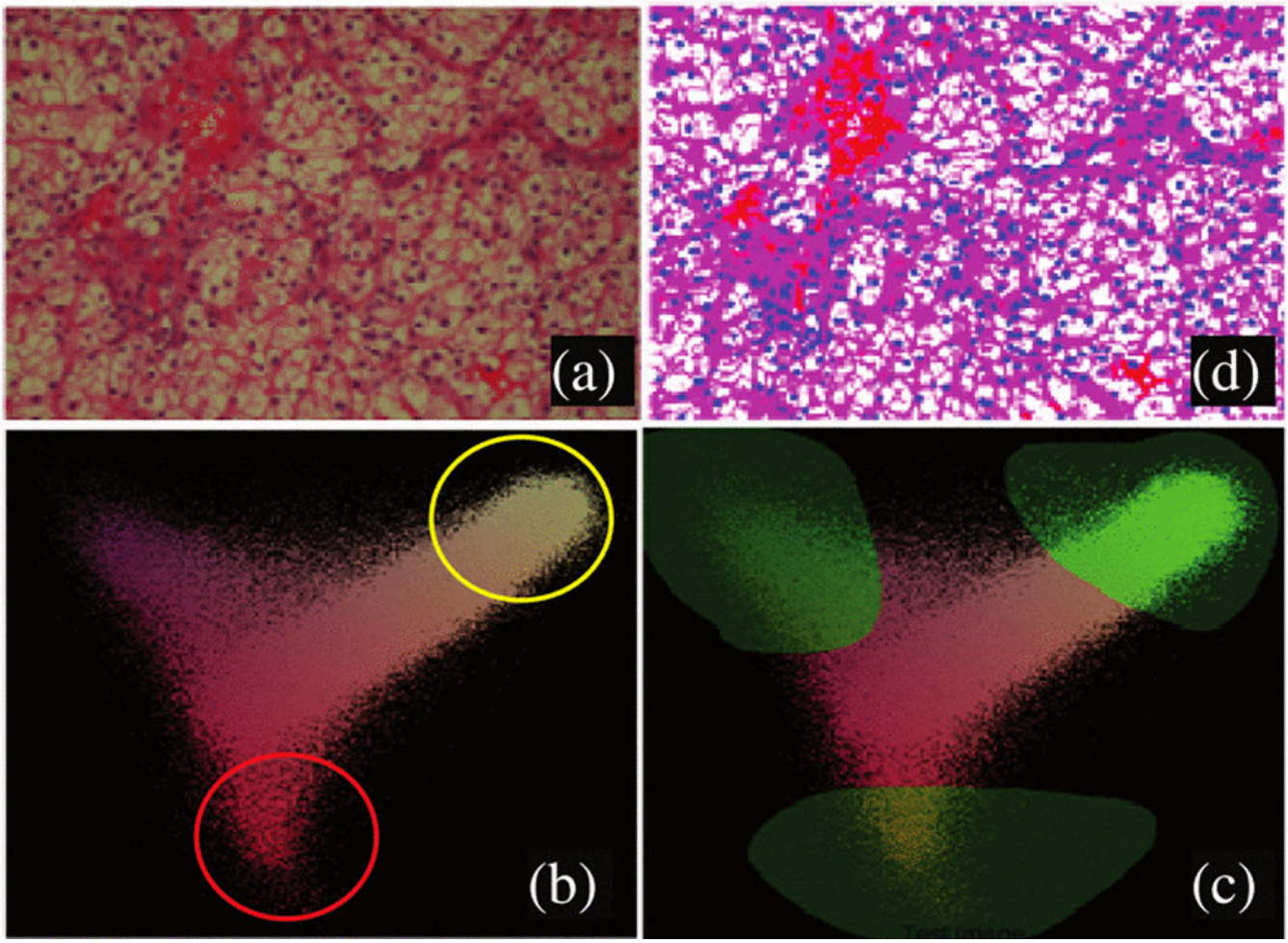

Figure 3.

(a) Test image (b) Random spread visualization showing dense regions corresponding to frequently occurring image pixels(c) User marked zones based on different color classes in test image. (d) Pseudo color segmentation results.

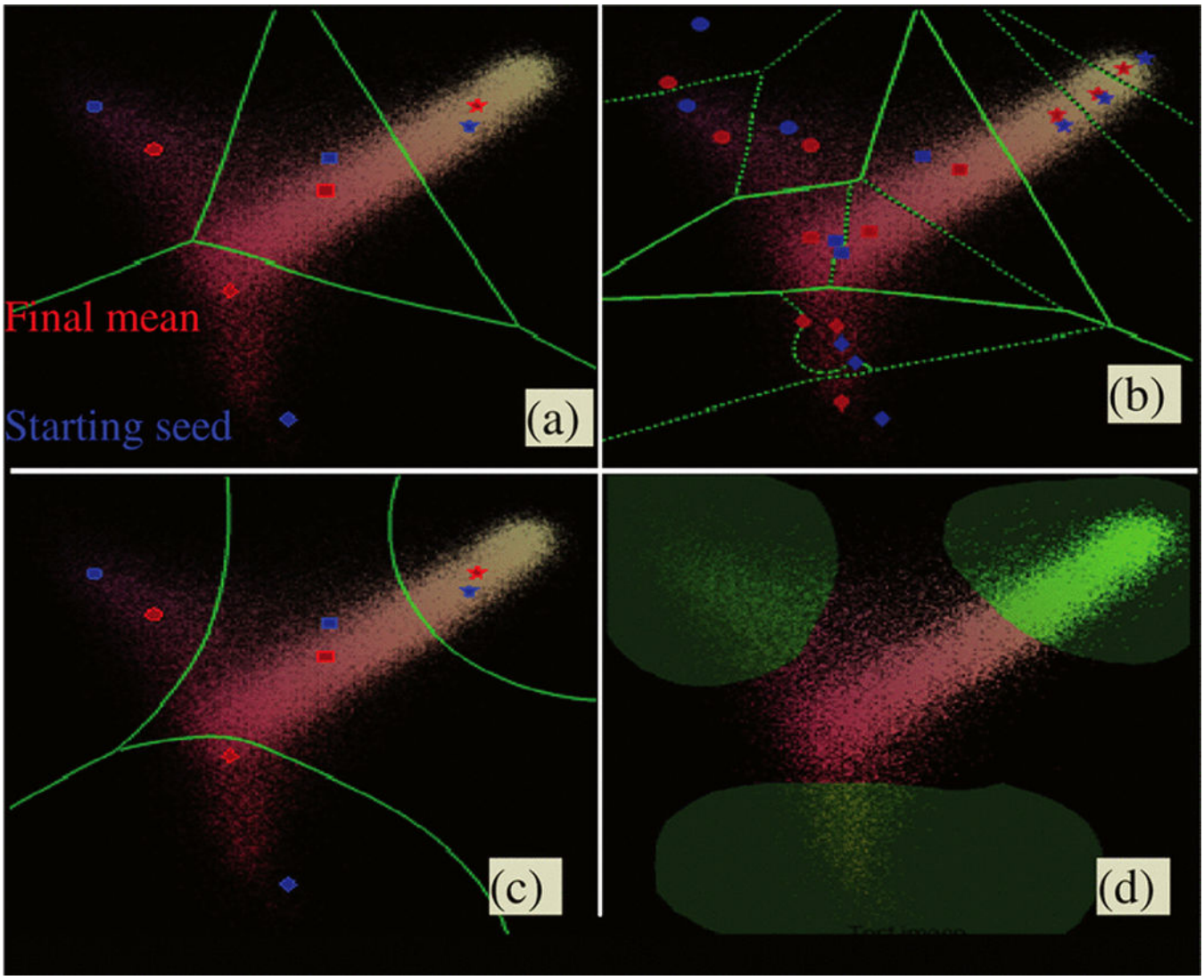

Figure 4.

(a) Class partitions shown for SK-means segmentation. (b) MSK-means multiple sub-classes can be combined to cater for intra-class variations. (c) WSK-means can change classification result by increasing and decreasing class zones based on slider weights. (d) Interactive Color map – user can select zones of any shape and size.

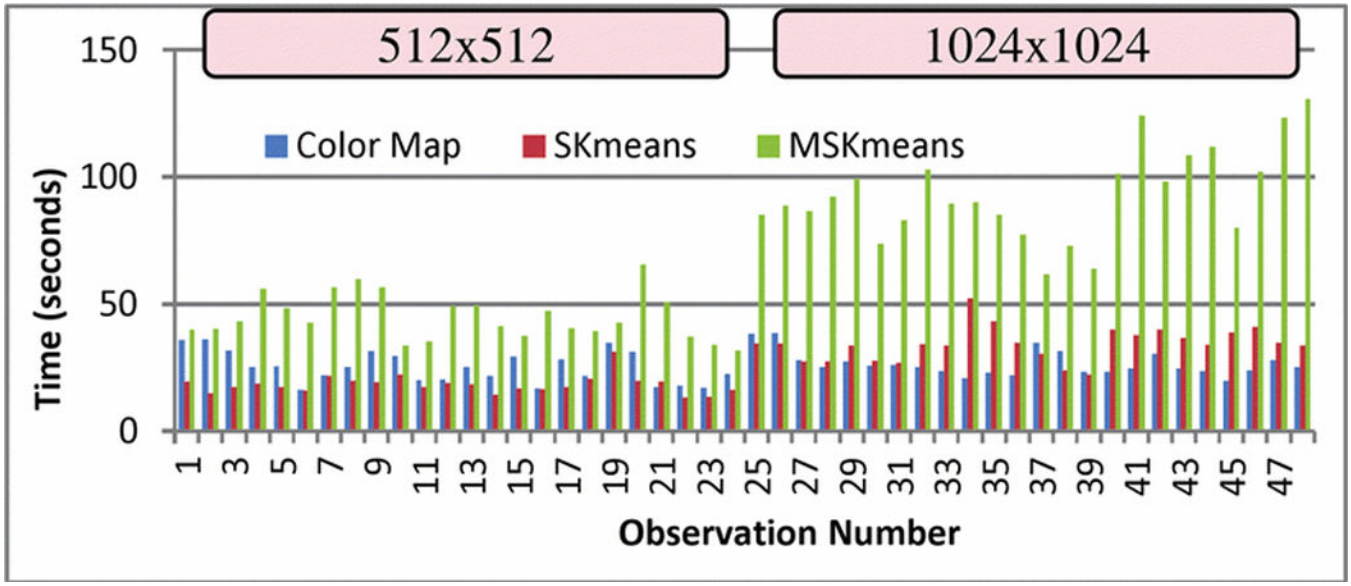

Figure 5.
User interaction time (including computation time) comparison for two sub groups. Color map segmentation performs better for larger images.

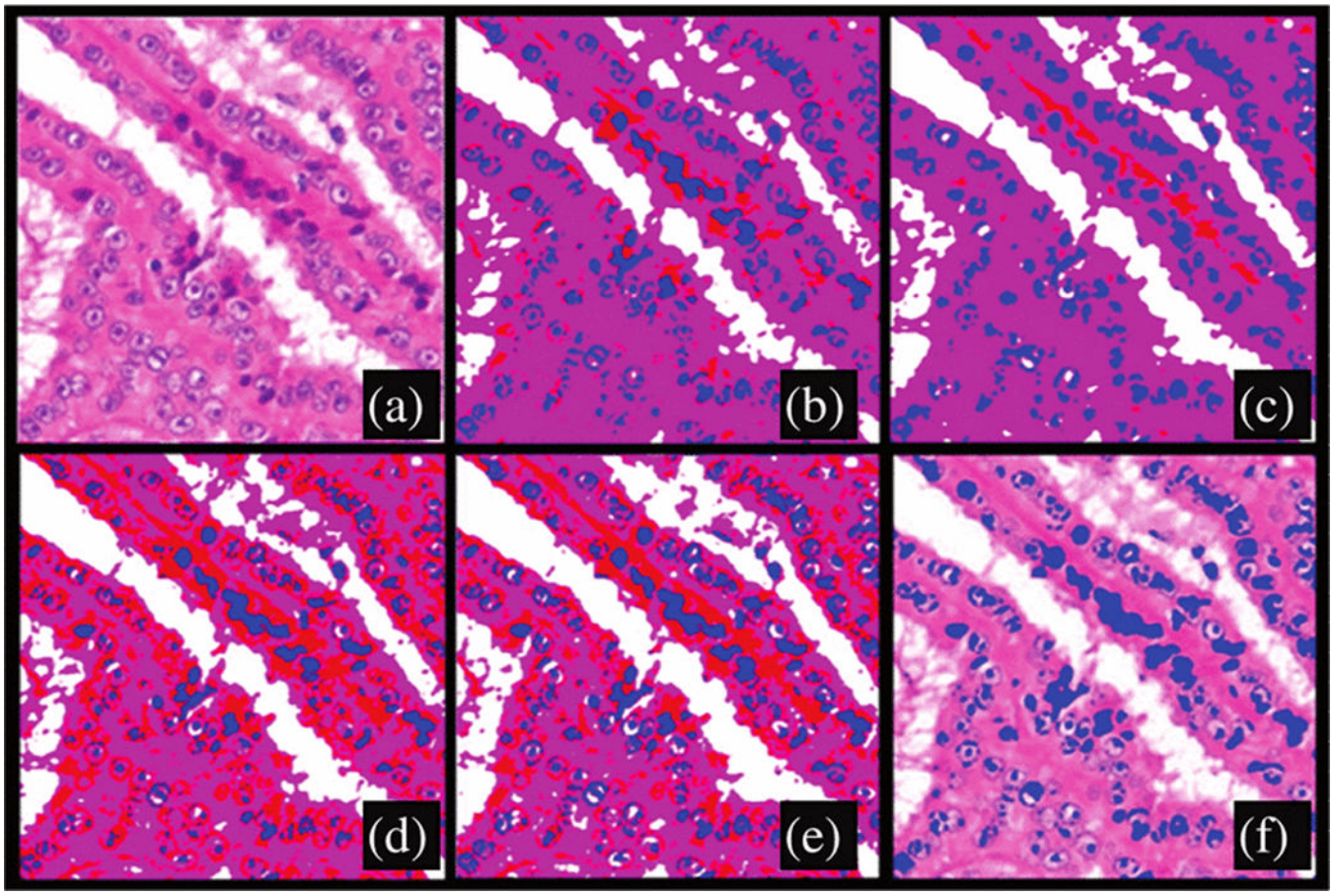

Figure 6.

(a) Test image (b) WSK-means segmentation used as reference (c) Color map based segmentation (d) SK-means segmentation (e) MSK-means segmentation (f) Level sets based segmentation for single class overlaid on top of test image

Table-1

User interaction time comparison

	Time (sees) μ±σ			
	Level sets (single class)	**Color maps**	**SK-means**	**MSK-means**
Images 512×512	150.78±46.01	25.04±6.26	18.23±3.60	44.87±9.08
Images 1024×1024	1593.82+39.77	26.48+5.09	34.19±6.79	91.28+16.60

Table-2

Segmentation accuracy comparison

	Accuracy (μ±σ)	Commissions (μ±σ)	Omissions (μ±σ)
WSK-means	1.0±0.0	0.0+0.0	0.0±0.0
Color Maps	0.874±0.06	0.126±0.06	0.126±0.057
SK-means	0.839±0.09	0.161±0.09	0.161±0.09
MSK-means	0.859±0.09	0.141±0.09	0.141±0.09
Level sets	0.977±0.02	0.083±0.04	0.023±0.02